4-2000

Probability Distribution of Distance in a Uniform Ellipsoid: Theory and Applications to Physics

Michelle Parry
Longwood University, parryml@longwood.edu

Ephraim Fischbach
Purdue University

Probability distribution of distance in a uniform ellipsoid: Theory and applications to physics

Michelle Parry[a)]
Department of Natural Sciences, Longwood College, Farmville, Virginia 23909

Ephraim Fischbach[b)]
Department of Physics, Purdue University, West Lafayette, Indiana 47907

(Received 4 November 1999; accepted for publication 24 November 1999)

A number of authors have previously found the probability $P_n(r)$ that two points uniformly distributed in an n-dimensional sphere are separated by a distance r. This result greatly facilitates the calculation of self-energies of spherically symmetric matter distributions interacting by means of an arbitrary radially symmetric two-body potential. We present here the analogous results for $P_2(r;\epsilon)$ and $P_3(r;\epsilon)$ which respectively describe an ellipse and an ellipsoid whose major and minor axes are $2a$ and $2b$. It is shown that for $\epsilon=(1-b^2/a^2)^{1/2}\leqslant 1$, $P_2(r;\epsilon)$ and $P_3(r;\epsilon)$ can be obtained as an expansion in powers of ϵ, and our results are valid through order ϵ^4. As an application of these results we calculate the Coulomb energy of an ellipsoidal nucleus, and compare our result to an earlier result quoted in the literature. © *2000 American Institute of Physics.* [S0022-2488(00)04304-8]

I. INTRODUCTION AND SUMMARY

It is well known that the exchange of fields with appropriate quantum numbers gives rise to two-body potentials $V(|\mathbf{r}_1-\mathbf{r}_2|)\equiv V(r)$ between particles 1 and 2, which contribute in turn to the self-energies of many-body systems such as nuclei and neutron stars. In typical applications of interest these potentials are often of the Yukawa form,

$$V(r)=C_{\mathrm{Y}}\frac{e^{-r/\lambda}}{r}, \tag{1.1}$$

where C_{Y} and λ are constants, or are inverse powers

$$V(r)=\frac{C_n}{r^n} \quad (n=1,2,3,\ldots), \tag{1.2}$$

where C_n is a constant. The most familiar example is the self-energy of a spherical charge distribution (e.g., a spherically symmetric nucleus) arising from the Coulomb potential

$$V_{\mathrm{C}}(r)=\frac{e^2}{|\mathbf{r}_1-\mathbf{r}_2|}\equiv\frac{e^2}{r}. \tag{1.3}$$

As we discuss in Sec. IV, the average interaction energy $U_{\mathrm{C}}\equiv\langle V_{\mathrm{C}}(r)\rangle$ of a single pair of charges having a uniform probability distribution in a sphere of radius R is given by

$$U_{\mathrm{C}}=\frac{6}{5}\frac{e^2}{R}. \tag{1.4}$$

For a nucleus containing Z charges, and hence $Z(Z-1)/2$ pairs, the total Coulomb energy is[1]

a)Electronic mail: mparry@longwood.lwc.edu
b)Electronic mail: ephraim@physics.purdue.edu

$$W_C=\frac{1}{2}Z(Z-1)U_C=\frac{3}{5}Z(Z-1)\frac{e^2}{R}. \tag{1.5}$$

The conventional way of obtaining U_C is to integrate $V_C(|\mathbf{r}_1-\mathbf{r}_2|)$ over $\mathbf{r}_1$ and $\mathbf{r}_2$ which requires evaluating a six-dimensional integral. For the Coulomb potential this is relatively straightforward, but for other potentials evaluating U_C is considerably more difficult, particularly for the inverse power potentials in Eq. (1.2). These typically arise from the simultaneous exchange of two quanta: For example, the exchange of two pseudoscalars produces a $1/r^3$ potential,[2–6] while the exchange of a neutrino–antineutrino pair leads to a $1/r^5$ potential.[7–10] Evaluation of U for these potentials in nuclei or neutron stars would lead to formally divergent integrals, but finite results are obtained by introducing the hard-core radius r_c, which cuts off the lower limit of integration. When the hard-core restriction $|\mathbf{r}_1-\mathbf{r}_2|<r_c$ is incorporated into the conventional evaluation of U, as in Eq. (4.3) below, it leads to complicated constraints on the six-dimensional integration region. By contrast, the same constraint can be expressed trivially in terms of the function $P_3(r)$ in Eq. (1.6), which gives the probability that two points in a sphere of radius R are separated by a distance $r\leqslant 2R$. The utility of this geometric probability approach lies not only in its ability to deal with the hard core constraint, but also in its universal applicability to any potential $V(r)$, as we discuss later.

The object of the present paper is to extend the above formalism to ellipsoids and ellipses, which would allow geometric probability techniques to be applied to systems in which there were deviations from exact spherical or circular symmetry. As in the case of the function $P_3(r)$, once the corresponding functions are determined for an ellipsoid or an ellipse, the evaluation of the self-energy U for an *arbitrary* two-body potential becomes trivial.

To set the stage for the ensuing discussion, we begin by reviewing earlier results for the probability distributions in spherically symmetric geometries. Consider two points 1 and 2 located at coordinates $\mathbf{r}_1$ and $\mathbf{r}_2$ in a uniformly distributed n-dimensional sphere of radius R, and let $r=|\mathbf{r}_1-\mathbf{r}_2|$. The normalized probability $P_n(r)$ that 1 and 2 are separated by a distance r, $0\leqslant r\leqslant 2R$, has been treated by Deltheil,[11] Hammersley,[12] Overhauser,[13] Lord,[14] and Parry[15] (see also Kendall, and Moran[16] and Santaló[17]). It is convenient to introduce the variable $s=r/2R$, $0\leqslant s\leqslant 1$, and to then define $P_n(s)$ as the normalized probability that s be in the interval $(s,s+ds)$. $P_n(s)$ is given by[17]

$$P_n(s)=2^n n s^{n-1} I_{1-s^2}\left(\frac{(n+1)}{2},\frac{1}{2}\right), \tag{1.6}$$

where $I_x(p,q)$ is the incomplete beta function,

$$I_x(p,q)=\frac{\Gamma(p+q)}{\Gamma(p)\Gamma(q)}\int_0^x dt\, t^{p-1}(1-t)^{q-1}. \tag{1.7}$$

As discussed here earlier and in Ref. 10, the results for $n=1,2,3$ are of interest in physics when calculating the self-energies of various configurations of charges, and hence we exhibit the explicit functional forms for $P_1(s)$, $P_2(s)$, and $P_3(s)$ below:

$$P_1(s)=2(1-s),$$

$$P_2(s)=\frac{16}{\pi}s[\cos^{-1}s-s(1-s^2)^{1/2}], \tag{1.8}$$

$$P_3(s)=12s^2(1-s)^2(2+s).$$

In terms of $P_n(s)$ the self-energy U of a one-, two-, or three-dimensional configuration of charges interacting via an arbitrary potential $V(s)$ is given by

$$U=\int_0^1 ds\, P_n(s)V(s). \tag{1.9}$$

The effects of the hard-core radius r_c can be included trivially by replacing the lower limit in Eq. (1.9) by $s_c=r_c/2R$.

For some applications where symmetry conditions are important, it is essential to know how the results in Eqs. (1.8) change in the presence of deviations from exact circular or spherical symmetry, characterized by a nonvanishing eccentricity ϵ. In what follows we derive the appropriate generalizations of $P_2(r)$ and $P_3(r)$ for an ellipse and an oblate spheroid, which we denote by $P_2(r;\epsilon)$ and $P_3(r;\epsilon)$, respectively. The outline of our paper is as follows. In Sec. II we present the (unpublished) Overhauser method for deriving $P_3(r)$, which we then generalize in Sec. III to obtain $P_3(r;\epsilon)$. The expression for $P_3(r;\epsilon)$ for an oblate spheroid is given in Eqs. (3.31)–(3.34), and analogous results for a prolate spheroid can then be obtained trivially. As an illustrative example, we use the results of Sec. III to calculate the Coulomb energy of an ellipsoidal nucleus in Sec. IV, and we compare our results to those obtained earlier by Feenberg.[18] In the Appendix we present the results for $P_2(r;\epsilon)$, which can be derived in analogy to $P_3(r;\epsilon)$, as discussed in Ref. 15.

II. THE METHOD OF OVERHAUSER

The results for $P_2(r;\epsilon)$ and $P_3(r;\epsilon)$ can be obtained using either the Hammersley[12] or Overhauser[13] method. The latter has a simple geometric interpretation which is discussed in greater detail in Ref. 15, and which we summarize below.

In a uniform three-dimensional sphere of radius R suppose that point 1 is located a distance ρ from the center of the sphere and that point 2 is located a distance r from point 1. The conditional probability that point 2 is located a distance r from point 1, given that point 1 is located a distance ρ from the origin of the sphere, is defined to be $f(r|\rho)$. Similarly, $f(\rho)$ is the probability that point 1 is located a distance ρ from the origin, where ρ and r are continuous random variables. Then,

$$P_3(r)\equiv f(r)=\int_0^R f(r|\rho)f(\rho)\,d\rho, \tag{2.1}$$

where $f(r)$ is the sought-after probability that the two points are separated by a distance r. Evidently,

$$f(\rho)d\rho=\frac{4\pi\rho^2 d\rho}{\frac{4}{3}\pi R^3}=\frac{3\rho^2 d\rho}{R^3} \tag{2.2}$$

for $0\leqslant\rho\leqslant R$. Since point 1 is required to be inside the sphere, $f(\rho)$ must be normalized such that

$$\int_0^R f(\rho)\,d\rho=\int_0^R \frac{3\rho^2}{R^3}d\rho=1. \tag{2.3}$$

It is convenient to calculate $f(r)$ separately for the two cases, $0\leqslant r\leqslant R$ and $R\leqslant r\leqslant 2R$. We show, however, that $f(r)$ has the same functional form for both regions.

When $0\leqslant r\leqslant R$, there are two regions of ρ in which $f(r|\rho)$ has different functional forms. From Fig. 1(a) it follows that when $0\leqslant\rho\leqslant R-r$,

$$f(r|\rho)dr=\frac{4\pi r^2 dr}{\frac{4}{3}\pi R^3}=\frac{3r^2 dr}{R^3}. \tag{2.4}$$

However, when $R-r\leqslant\rho\leqslant R$, the shell intersects the sphere as in Fig. 1(b). In this case the enclosed surface area (S) is no longer $4\pi r^2$, but is given by

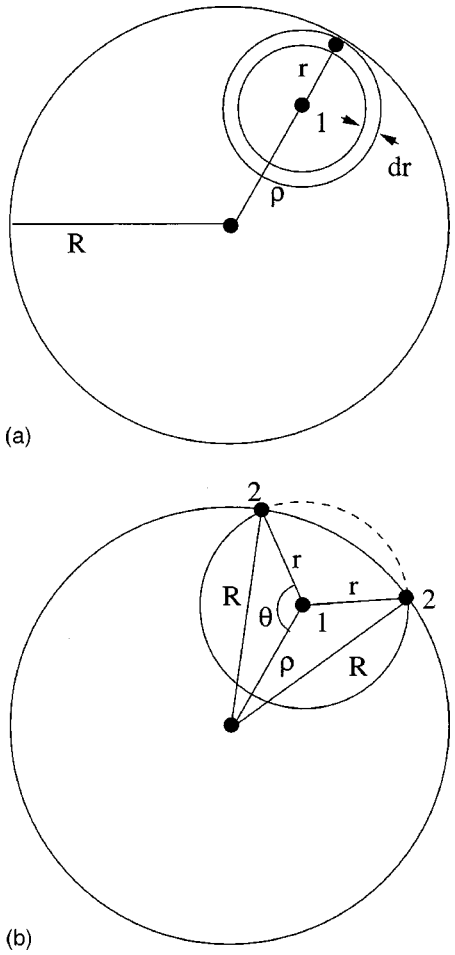

FIG. 1. (a) (top) Geometry for the Overhauser method when $0 \leqslant r \leqslant R$ and $0 \leqslant \rho \leqslant R-r$. Point 2 is constrained to lie on the surface of a spherical shell of radius r centered at point 1. Note that the spherical shell is totally enclosed in the sphere. (b) (bottom) Geometry for the case $0 \leqslant r \leqslant R$ and $R-r \leqslant \rho \leqslant R$. The spherical shell made by point 2 intersects the sphere at an angle θ. The dashed line represents the portion of the spherical shell that lies outside the sphere.

$$S_{\text{enclosed}} = r^2 \int_0^{2\pi} d\phi' \int_0^{\theta} \sin\theta'\, d\theta' = 2\pi r^2 (1-\cos\theta) = 2\pi r^2 \left[1 - \frac{\rho^2 + r^2 - R^2}{2\rho r} \right], \tag{2.5}$$

where the law of cosines has been used to replace $\cos\theta$. Hence,

$$f(r|\rho)dr = \frac{3}{2}\frac{r^2}{R^3}\left(1 - \frac{\rho^2 + r^2 - R^2}{2\rho r} \right) dr, \tag{2.6}$$

for $R-r \leqslant \rho \leqslant R$. Combining Eqs. (2.1), (2.2), (2.4), and (2.6) yields

$$\begin{aligned} P_3(r) \equiv f(r) &= \int_0^{R-r} \left(\frac{3\rho^2}{R^3} \right) \left(\frac{3r^2}{R^3} \right) d\rho + \int_{R-r}^{R} \left(\frac{3\rho^2}{R^3} \right) \left[\frac{3}{2}\frac{r^2}{R^3} \left(1 - \frac{\rho^2 + r^2 - R^2}{2\rho r} \right) \right] d\rho \\ &= \frac{3r^2}{R^3} - \frac{9}{4}\frac{r^3}{R^4} + \frac{3}{16}\frac{r^5}{R^6}. \end{aligned} \tag{2.7}$$

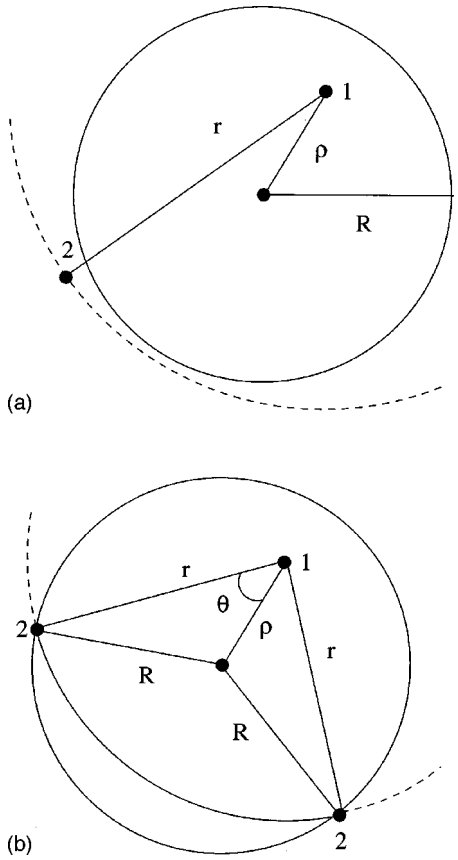

FIG. 2. (a) (top) Geometry for the case $R \leqslant r \leqslant 2R$ and $0 \leqslant \rho \leqslant r-R$. The spherical shell is always outside the sphere when $0 \leqslant \rho \leqslant r-R$. The dashed line (only part of which is shown) represents the portion of the spherical shell that lies outside the sphere. (b) (bottom) Geometry for the case when $R \leqslant r \leqslant 2R$ and $r-R \leqslant \rho \leqslant R$. The spherical shell made by point 2 intersects the sphere at an angle θ.

When $R \leqslant r \leqslant 2R$ there are also two regions of ρ in which $f(r|\rho)$ has different functional forms. The spherical shell lies outside the given sphere when $0 \leqslant \rho \leqslant r-R$ as seen in Fig. 2(a), and hence

$$f(r|\rho)=0. \tag{2.8}$$

When $r-R \leqslant \rho \leqslant R$ the spherical shell intersects the sphere as in Fig. 2(b). The discussion leading to Eq. (2.6) can be taken over immediately and we find for $r-R \leqslant \rho \leqslant R$,

$$f(r|\rho)\,dr=\frac{3}{2}\frac{r^2}{R^3}\left(1-\frac{\rho^2+r^2-R^2}{2\rho r}\right)dr. \tag{2.9}$$

Combining Eqs. (2.1), (2.2), (2.8), and (2.9) yields

$$\begin{aligned} P_3(r)\equiv f(r)&=\int_0^{r-R}\left(\frac{3\rho^2}{R^3}\right)(0)\,d\rho+\int_{r-R}^{R}\left(\frac{3\rho^2}{R^3}\right)\left[\frac{3}{2}\frac{r^2}{R^3}\left(1-\frac{\rho^2+r^2-R^2}{2\rho r}\right)\right]d\rho \\ &=\frac{3r^2}{R^3}-\frac{9}{4}\frac{r^3}{R^4}+\frac{3}{16}\frac{r^5}{R^6} \end{aligned} \tag{2.10}$$

for $R \leqslant r \leqslant 2R$. We observe from Eqs. (2.7) and (2.10) that the probability function $P_3(r) \equiv f(r)$ has the same functional form over the entire region of r, and agrees with the results obtained previously by Deltheil,[11] Hammersley,[12] and Lord.[14] $P_3(r)dr$ in Eq. (2.10) reproduces the expression for $P_3(s)ds$ in Eq. (1.8) using $s = r/2R$. We note in passing that

$$\int_0^{2R} f(r)\, dr = 1, \tag{2.11}$$

which is the required normalization condition.

III. DISTRIBUTION OF DISTANCE IN AN OBLATE SPHEROID

A. General considerations

The equation for an oblate spheroid in Cartesian coordinates is

$$\frac{x^2}{a^2} + \frac{y^2}{a^2} + \frac{z^2}{b^2} = 1, \tag{3.1}$$

where a and b are the major and minor semi-axes, respectively. It is more convenient to describe the oblate spheroid in spherical coordinates $(\mathcal{R},\Theta,\Phi)$ so that the equation for the oblate spheroid may be written as

$$\mathcal{R}(\Theta,\Phi) = \frac{a\sqrt{1-\epsilon^2}}{\sqrt{1-\epsilon^2 \sin^2 \Theta}}, \tag{3.2}$$

where the eccentricity, ϵ, is defined to be

$$\epsilon = \sqrt{1 - \frac{b^2}{a^2}}. \tag{3.3}$$

It should be noted that $\mathcal{R}(\Theta,\Phi)$ is independent of the azimuthal angle Φ, and hence $\mathcal{R}(\Theta,\Phi) = \mathcal{R}(\Theta)$. Although the oblate spheroid can be described using any two of the three variables a, b, and ϵ, it is most convenient to use a and ϵ, since the maximum possible distance between two points in the oblate spheroid is $2a$.

Suppose that point 1 is located at a position (ρ,θ), where ρ is the distance from the origin of the oblate spheroid and θ is the angle with respect to the z axis. If point 2 is a distance r from point 1 as in Fig. 3(a), then it is constrained to lie on the surface of a sphere with radius r. The probability that point 1 is located at (ρ,θ) is defined as $P(\rho,\theta)$, and the conditional probability that point 2 is located a distance r from point 1, given that point 1 is located at a position (ρ,θ), is $P(r|\rho,\theta)$. $P(r;\epsilon)$ is then given by

$$P(r;\epsilon) = \int_0^{\pi} d\theta \int_0^{\mathcal{R}(\theta)} d\rho\, P(r|\rho,\theta) P(\rho,\theta), \tag{3.4}$$

where $P(r;\epsilon) \equiv P_3(r;\epsilon)$ is the probability that two points are separated by a distance r in a uniformly distributed oblate spheroid with eccentricity ϵ. Since point 1 is constrained to lie on the circumference of a circle of radius $\rho \sin\theta$, as shown in Fig. 3(b), it follows that

$$P(\rho,\theta)\, d\rho\, d\theta = \frac{3}{2} \frac{\rho \sin\theta}{a^3\sqrt{1-\epsilon^2}} d\rho\, \rho\, d\theta \tag{3.5}$$

for $0 \leqslant \rho \leqslant \mathcal{R}(\theta)$. The conditional probability $P(r|\rho,\theta)$ is proportional to the surface area (enclosed in the oblate spheroid) of the spherical shell made by point 2 as it rotates about point 1. It

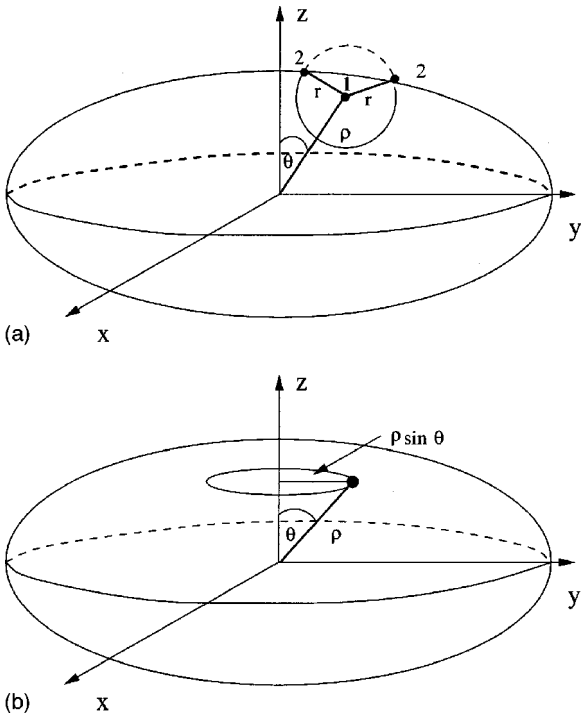

FIG. 3. (a) (top) Geometry of an oblate spheroid. Point 1 is at a distance ρ from the origin and located at an angle θ as shown. Point 2 is a distance r from 1. (b) (bottom) Constraint for $P(\rho,\theta)$ in an oblate spheroid. Point 1 is constrained to lie on a circle of radius $\rho \sin \theta$.

follows that $P(r|\rho,\theta)$ has a different functional form in each of four regions of r (i.e., ranges of values of r). When $0 \leqslant r \leqslant b$, the spherical shell can either be totally enclosed in the oblate spheroid or can intersect it. When $b \leqslant r \leqslant a$, the spherical shell always intersects the oblate spheroid. When $a \leqslant r \leqslant 2b$, the spherical shell can either be outside the oblate spheroid or can intersect it. Finally, when $2b \leqslant r \leqslant 2a$, the spherical shell can either be totally outside the oblate spheroid or it can intersect the oblate spheroid only over a certain region of θ. $P(r;\epsilon)$ cannot be expected *a priori* to have the same functional form over the entire range of values of r, and for this reason each of the above cases must be considered separately. We illustrate our formalism by considering the region $0 \leqslant r \leqslant b$.

B. The intersection of a sphere and an oblate spheroid

Since the probability function $P(r|\rho,\theta)$ is proportional to the surface area of the sphere of radius r enclosed in the oblate spheroid, one must determine how an oblate spheroid and a sphere intersect. The surface area of the sphere enclosed in the ellipsoid can be determined by introducing a new coordinate system (x',y',z') centered at point 1. The x' axis points in the same direction as the x axis, out of the page. The z' axis points toward the origin of the original coordinate system along ρ. Finally, the y' axis is perpendicular to the x' and z' axes. Associated with this new coordinate system are the spherical coordinates (r,θ',ϕ'). The surface area of the sphere enclosed in the oblate spheroid is then determined by

$$S_{\text{enclosed}} = r^2 \int d\phi' \int d(\cos\theta'), \tag{3.6}$$

where the limits of integration depend on how the sphere and the oblate spheroid intersect.

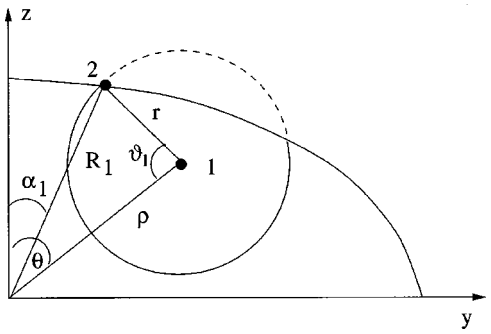

FIG. 4. One configuration illustrating the intersection of a sphere and an oblate spheroid. The dotted line represents the portion of the spherical shell that lies outside of the oblate spheroid. R_1 is the distance from the origin to the surface of the oblate spheroid at the location of the intersection, and is described by an angle α_1 according to Eq. (3.7). The angle ϑ_1 represents the position of intersection.

Consider the case $0 \leqslant r \leqslant b$, for which there are two subcases. In the first subcase the sphere intersects the oblate spheroid as in Fig. 4 which, for simplicity, depicts only one quadrant of the oblate spheroid. In this figure, $\mathcal{R}_1 = \mathcal{R}(\alpha_1)$ describes the position of point 2 on the surface of the oblate spheroid and is given by

$$\mathcal{R}_1 = \mathcal{R}(\alpha_1) = \frac{a\sqrt{1-\epsilon^2}}{\sqrt{1-\epsilon^2 \sin^2 \alpha_1}}. \tag{3.7}$$

The surface area of the sphere enclosed in the oblate spheroid for this subcase is

$$S_{\text{enclosed}} = r^2 \int_0^{2\pi} d\phi' \int_{\cos \vartheta_1}^{1} d(\cos \theta') = \int_0^{2\pi} r^2 (1 - \cos \vartheta_1)\, d\phi'. \tag{3.8}$$

The integration over ϕ' is nontrivial since $\vartheta_1 = \vartheta_1(\phi')$, and will be discussed below.

In the second subcase $\mathcal{R}_2 = \mathcal{R}(\alpha_2)$ and $\mathcal{R}_3 = \mathcal{R}(\alpha_3)$ represent the positions of intersection and are defined in the same manner as above. In this case the surface area of the sphere enclosed in the oblate spheroid is

$$\begin{aligned} S_{\text{enclosed}} &= r^2 \int_0^{2\pi} d\phi' \int_{-1}^{\cos \vartheta_3} d(\cos \theta') + r^2 \int_0^{2\pi} d\phi' \int_{\cos \vartheta_2}^{1} d(\cos \theta') \\ &= 4\pi r^2 + r^2 \int_0^{2\pi} (\cos \vartheta_3 - \cos \vartheta_2)\, d\phi'. \end{aligned} \tag{3.9}$$

To determine $P(r;\epsilon)$, $\cos \vartheta_i$ $(i = 1,2,3)$ must be expressed in terms of the positions of intersection $\mathcal{R}_i$ which depend on the angles α_i explicitly as in Fig. 4. $\cos \vartheta_i$ can be expressed in terms of $\mathcal{R}_i$ using the law of cosines,

$$\cos \vartheta_i = \frac{\rho^2 + r^2 - \mathcal{R}_i^2}{2\rho r}. \tag{3.10}$$

Equation (3.10) does not give a total representation of the angle ϑ_i since $\mathcal{R}_i$ itself depends on the unknown angle α_i. This makes it necessary to find a second relationship between the angles ϑ_i and α_i.

Consider the triangle formed by ρ, r, and $\mathcal{R}_i$ and its relationship to the z axis of the defined coordinate system. From Fig. 5,

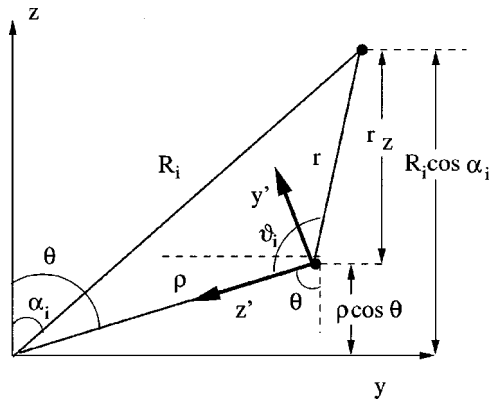

FIG. 5. Enlargement of Fig. 4 showing the primed coordinate system used to calculate the enclosed surface area. See text for further details.

$$\mathcal{R}_i \cos \alpha_i = \rho \cos \theta + r_z = \rho \cos \theta + r \sin \phi' \sin \vartheta_i \sin \theta - r \cos \vartheta_i \cos \theta. \tag{3.11}$$

Combining Eqs. (3.10) and (3.11) gives a quartic equation in $\cos \vartheta_i$ whose solution can be expressed as a series in powers of ϵ:

$$\begin{aligned}\cos \vartheta_i = Y &+ \frac{\epsilon^2}{2\rho r}[a^2 \cos^2 \theta + r^2(1-Y^2)(\sin^2 \phi' \sin^2 \theta - \cos^2 \theta)] \\ &+ \frac{\epsilon^4}{4\rho^2 r^2}[2\rho r a^2 \cos^2 \theta \sin^2 \theta + 2r^2 a^2 Y(\cos^4 \theta - 3 \sin^2 \phi' \sin^2 \theta \cos^2 \theta) \\ &+ 2\rho r^3(1-Y^2)(\sin^2 \phi' \sin^4 \theta - \sin^2 \theta \cos^2 \theta - 2 \sin^2 \phi' \sin^2 \theta \cos^2 \theta) \\ &+ 2r^4 Y(1-Y^2)(6 \sin^2 \phi' \sin^2 \theta \cos^2 \theta - \sin^4 \phi' \sin^4 \theta - \cos^4 \theta)] + 0(\epsilon^6) \\ &+ \cdots,\end{aligned} \tag{3.12}$$

$$Y = \frac{\rho^2 + r^2 - a^2}{2\rho r}, \tag{3.13}$$

where ... denotes terms of order ϵ^2 and ϵ^4 which do not contribute to the surface area. Note that $\cos \vartheta_i$ has the same functional form for $i = 1,2,3$, and hence we drop the subscript i.

For $0 \leqslant r \leqslant b$ there are thus two possibilities for the intersection of the sphere and the ellipsoid. For the purpose of calculating the surface area, the sphere is effectively (i.e., to order ϵ^4) totally enclosed in the oblate spheroid for $0 \leqslant \rho \leqslant \mathcal{R} - r$, which gives

$$S_{\text{enclosed}} = 4\pi r^2. \tag{3.14}$$

However, when $\mathcal{R} - r \leqslant \rho \leqslant \mathcal{R}$ the sphere intersects the oblate spheroid and produces a surface area equal to

$$S_{\text{enclosed}} = \int_0^{2\pi} r^2(1 - \cos \vartheta)\, d\phi'. \tag{3.15}$$

When the expression for $\cos \vartheta$ in Eq. (3.12) is substituted into the above result and the integration is carried out, we find

$$S_{\text{enclosed}}=2\pi r^2\Bigg\{(1-Y)-\frac{\epsilon^2}{2\rho r}\Bigg[a^2\cos^2\theta+r^2(1-Y^2)\Big(\frac{1}{2}\sin^2\theta-\cos^2\theta\Big)\Bigg]$$
$$-\frac{\epsilon^4}{4\rho^2r^2}\Bigg[2\rho r a^2\sin^2\theta\cos^2\theta+2r^2a^2Y\Big(-\frac{3}{2}\cos^2\theta+\frac{5}{2}\cos^4\theta\Big)+2\rho r^3(1-Y^2)$$
$$\times\Big(\frac{5}{2}\cos^4\theta-3\cos^2\theta+\frac{1}{2}\Big)+2r^4Y(1-Y^2)\Big(-\frac{35}{8}\cos^4\theta+\frac{15}{4}\cos^2\theta-\frac{3}{8}\Big)\Bigg]\Bigg\}. \quad (3.16)$$

The calculation of the intersection of a sphere and an oblate spheroid for the case in which $b\leqslant r\leqslant 2a$ can be carried out in an analogous manner, and leads to the same result as in Eq. (3.16) above. It follows that when the spherical shell and the oblate spheroid intersect, the surface area is independent of the regions of r and is always given by Eq. (3.16). The conditional probability $P(r|\rho,\theta)$ is then given by

$$P(r|\rho,\theta)=\frac{S_{\text{enclosed}}}{(4/3)\pi a^3\sqrt{1-\epsilon^2}}, \quad (3.17)$$

where the denominator is the volume of the ellipsoid. $P(r|\rho,\theta)$ is explicitly given in Eqs. (3.18)–(3.20) below.

C. The determination of $P(r;\epsilon)$

We begin by summarizing the three possible functional forms for $P(r|\rho,\theta)$. When $0\leqslant r\leqslant b$ and $0\leqslant\rho\leqslant\mathcal{R}-r$, the sphere is effectively totally enclosed in the oblate spheroid, and hence the contribution to $P(r|\rho,\theta)$ is

$$P(r|\rho,\theta)=\frac{3r^2}{a^3\sqrt{1-\epsilon^2}}. \quad (3.18)$$

When the sphere intersects the oblate spheroid for $0\leqslant r\leqslant b$, $\mathcal{R}-r\leqslant\rho\leqslant\mathcal{R}$, and $a\leqslant r\leqslant 2b$, $r-\mathcal{R}\leqslant\rho\leqslant\mathcal{R}$, the contribution to $P(r|\rho,\theta)$ is

$$P(r|\rho,\theta)=\frac{3}{2}\frac{r^2}{a^3\sqrt{1-\epsilon^2}}\Bigg\{(1-Y)-\frac{\epsilon^2}{2\rho r}\Bigg[a^2\cos^2\theta+r^2(1-Y^2)\Big(\frac{1}{2}-\frac{3}{2}\cos^2\theta\Big)\Bigg]$$
$$-\frac{\epsilon^4}{4\rho^2r^2}\Bigg[2\rho r a^2\sin^2\theta\cos^2\theta+r^2a^2Y(-3\cos^2\theta+5\cos^4\theta)$$
$$+\rho r^3(1-Y^2)(5\cos^4\theta-6\cos^2\theta+1)$$
$$+\frac{1}{4}r^4Y(1-Y^2)(-35\cos^4\theta+30\cos^2\theta-3)\Bigg]\Bigg\}. \quad (3.19)$$

Finally, when $a\leqslant r\leqslant 2b$, and $0\leqslant\rho\leqslant r-\mathcal{R}$, the sphere is effectively totally outside the oblate spheroid, and hence the contribution to $P(r|\rho,\theta)$ is

$$P(r|\rho,\theta)=0. \quad (3.20)$$

The functional forms of $P(r|\rho,\theta)$ and $P(\rho,\theta)$ can be used to determine $P(r;\epsilon)$. Since $P(r|\rho,\theta)$ has only been determined for the upper half of the oblate spheroid, which is specified by point 1 in the the range $0\leqslant\theta\leqslant\pi/2$, the corresponding contribution to $P(r;\epsilon)$ for point 1 lying in the upper half of the oblate spheroid is given by

$$P(r;\epsilon)_{\text{upper}}=\int_0^{\pi/2} d\theta \int_0^{\mathcal{R}} d\rho\, P(r|\rho,\theta)P(\rho,\theta). \tag{3.21}$$

Similarly, the contribution from the lower half of the oblate spheroid is given by

$$P(r;\epsilon)_{\text{lower}}=\int_{\pi/2}^{\pi} d\theta \int_0^{\mathcal{R}} d\rho\, P(r|\rho,\theta)P(\rho,\theta), \tag{3.22}$$

so that

$$P(r;\epsilon)=P(r;\epsilon)_{\text{upper}}+P(r;\epsilon)_{\text{lower}}. \tag{3.23}$$

On symmetry grounds it follows that

$$P(r;\epsilon)_{\text{upper}}=P(r;\epsilon)_{\text{lower}}, \tag{3.24}$$

which implies that

$$P(r;\epsilon)=2P(r;\epsilon)_{\text{upper}}. \tag{3.25}$$

In analogy to the case of the sphere treated in Sec. II, $P(r;\epsilon)$ can be obtained by evaluating it separately in each of four regions of the variable r. For $0\leqslant r\leqslant b$ the sphere is effectively totally enclosed in the oblate spheroid in a region where $0\leqslant\rho\leqslant\mathcal{R}-r$, and it intersects the oblate spheroid in a region where $\mathcal{R}-r\leqslant\rho\leqslant\mathcal{R}$. Using the results of Eqs. (3.5), (3.18), (3.19), (3.21), and (3.25),

$$\begin{aligned}
P(r;\epsilon)_{\text{upper}}=\frac{1}{2}P(r;\epsilon)=&\int_0^{\pi/2}\int_0^{\mathcal{R}-r} d\rho\, d\theta\left(\frac{3\rho^2\sin\theta}{2a^3\sqrt{1-\epsilon^2}}\right)\left(\frac{3r^2}{a^3\sqrt{1-\epsilon^2}}\right)\\
&+\int_0^{\pi/2}\int_{\mathcal{R}-r}^{\mathcal{R}} d\rho\, d\theta\left(\frac{3\rho^2\sin\theta}{2a^3\sqrt{1-\epsilon^2}}\right)\left(\frac{3r^2}{2a^3\sqrt{1-\epsilon^2}}\right)\left\{(1-Y)-\frac{\epsilon^2}{2\rho r}\left[a^2\cos^2\theta\right.\right.\\
&+r^2(1-Y^2)\left(\frac{1}{2}-\frac{3}{2}\cos^2\theta\right)\Big]-\frac{\epsilon^4}{4\rho^2r^2}\Big[2\rho r a^2\sin^2\theta\cos^2\theta\\
&+r^2a^2Y(-3\cos^2\theta+5\cos^4\theta)+\rho r^3(1-Y^2)(5\cos^4\theta-6\cos^2\theta+1)\\
&\left.\left.+\frac{1}{4}r^4Y(1-Y^2)(-35\cos^4\theta+30\cos^2\theta-3)\Big]\right\},
\end{aligned} \tag{3.26}$$

where

$$\mathcal{R}=\mathcal{R}(\theta)=\frac{a\sqrt{1-\epsilon^2}}{\sqrt{1-\epsilon^2\sin^2\theta}}. \tag{3.27}$$

Among the terms appearing in Eq. (3.26), several do not contribute to order ϵ^4. These are given by

$$\int_0^1 \int_{a-r}^{a} d\rho\, d(\cos\theta) \left(\frac{3\rho^2}{2a^3\sqrt{1-\epsilon^2}} \right) \left(\frac{3r^2}{2a^3\sqrt{1-\epsilon^2}} \right) \left(\frac{-\epsilon^4}{4\rho^2 r^2} \right)$$
$$\times \left\{ r^2 a^2 Y(-3\cos^2\theta + 5\cos^4\theta) + \rho r^3 (1-Y^2)(5\cos^4\theta - 6\cos^2\theta + 1) \right.$$
$$\left. + \frac{1}{4} r^4 Y(1-Y^2)(-35\cos^4\theta + 30\cos^2\theta - 3) \right\}. \tag{3.28}$$

Notice that to order ϵ^4, the limits on the ρ integration can be replaced by $a-r$ and a, respectively. From Eq. (3.26),

$$P(r;\epsilon)_{\text{upper}} = \frac{1}{2} P(r;\epsilon) = \int_0^1 d(\cos\theta) \frac{9r^2}{4a^6(1-\epsilon^2)} \left\{ \frac{1}{6}\mathcal{R}^3 - \frac{1}{4}\mathcal{R}^2 r + \frac{1}{24} r^3 + \frac{1}{2}\mathcal{R}a^2 - \frac{1}{4} r a^2 \right.$$
$$+ \epsilon^2 \left(-\frac{1}{2} a^2 \mathcal{R} + \frac{1}{4} r a^2 \cos^2\theta \right) + \epsilon^2 \left(\frac{1}{4} - \frac{3}{4}\cos^2\theta \right)$$
$$\times \left[\frac{1}{4}\mathcal{R}^3 + \frac{3}{16} r^3 - \frac{1}{4}\mathcal{R} r^2 - \frac{3}{8}\mathcal{R}^2 r - \frac{1}{2}\mathcal{R}a^2 + \frac{1}{4} r a^2 \right.$$
$$\left. \left. - \frac{1}{4} \frac{(r^2-a^2)^2}{r} \ln\left(1 - \frac{r}{\mathcal{R}} \right) \right] + \epsilon^4 \sin^2\theta \cos^2\theta \left(-\frac{1}{2}\mathcal{R}a^2 + \frac{1}{4} r a^2 \right) \right\}. \tag{3.29}$$

The integration over $\cos\theta$ can be carried out by combining Eq. (3.27) and the results for various useful integrals which are tabulated in Ref. 15. We find to order ϵ^4,

$$P(r;\epsilon) = \left(3\frac{r^2}{a^3} - \frac{9}{4}\frac{r^3}{a^4} + \frac{3}{16}\frac{r^5}{a^6} \right) + \epsilon^2 \left(\frac{3}{2}\frac{r^2}{a^3} - \frac{3}{2}\frac{r^3}{a^4} + \frac{3}{16}\frac{r^5}{a^6} \right)$$
$$+ \epsilon^4 \left(\frac{9}{8}\frac{r^2}{a^3} - \frac{27}{20}\frac{r^3}{a^4} + \frac{9}{40}\frac{r^5}{a^6} \right) + O(\epsilon^6). \tag{3.30}$$

Although this probability function is valid for only one region of r $(0 \leqslant r \leqslant b)$, the analogous results for the other three regions can be obtained in a similar manner.[15]

D. Final results

Although we have argued that the functional form of $P(r;\epsilon)$ could be different in each of the four regions $0 \leqslant r \leqslant b$, $b \leqslant r \leqslant a$, $a \leqslant r \leqslant 2b$, and $2b \leqslant r \leqslant 2a$, it turns out that the first three regions are in fact described by the expression given in Eq. (3.30). Hence the final expression for $P(r;\epsilon)$ is

$$P(r;\epsilon) = \begin{cases} P_{\text{I}}(r;\epsilon), & 0 \leqslant r \leqslant 2b, \\ P_{\text{II}}(r;\epsilon), & 2b \leqslant r \leqslant 2a, \end{cases} \tag{3.31}$$

where

$$P_{\text{I}}(r;\epsilon) = \left(3\frac{r^2}{a^3} - \frac{9}{4}\frac{r^3}{a^4} + \frac{3}{16}\frac{r^5}{a^6} \right) + \epsilon^2 \left(\frac{3}{2}\frac{r^2}{a^3} - \frac{3}{2}\frac{r^3}{a^4} + \frac{3}{16}\frac{r^5}{a^6} \right)$$
$$+ \epsilon^4 \left(\frac{9}{8}\frac{r^2}{a^3} - \frac{27}{20}\frac{r^3}{a^4} + \frac{9}{40}\frac{r^5}{a^6} \right) + O(\epsilon^6) \tag{3.32}$$

and

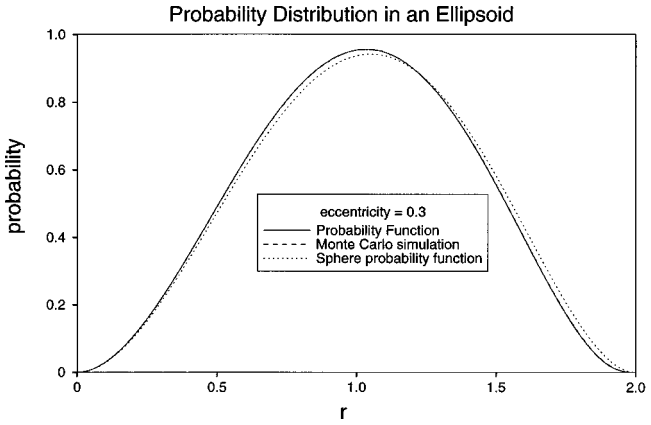

FIG. 6. A plot of probability function $P_3(r;\epsilon)$ as a function of r for an ellipsoid with $a=1.0$ and $\epsilon=0.3$. The solid line is the analytic function in Eqs. (3.31)–(3.34). Also shown (but not visible) is a Monte Carlo simulation of $P_3(r;\epsilon)$ which is indistinguishable from the analytic result. Note that the result for the ellipsoid differs from that for a sphere with radius $a=1.0$, which is shown by the dotted line.

$$
\begin{aligned}
P_{\mathrm{II}}(r;\epsilon)=X\Bigg\{&\left(3\frac{r^2}{a^3}-\frac{9}{4}\frac{r^3}{a^4}+\frac{3}{16}\frac{r^5}{a^6}\right)+\epsilon^2\left(\frac{3}{2}\frac{r^2}{a^3}-\frac{3}{2}\frac{r^3}{a^4}+\frac{3}{16}\frac{r^5}{a^6}\right)+\epsilon^4\left(\frac{9}{8}\frac{r^2}{a^3}-\frac{27}{20}\frac{r^3}{a^4}+\frac{9}{40}\frac{r^5}{a^6}\right)\Bigg\}\\
&+\epsilon^2X(1-X^2)\left\{\frac{117}{96}\frac{r^2}{a^3}-\frac{171}{192}\frac{r^3}{a^4}-\frac{9}{32}\frac{r^4}{a^5}+\frac{27}{128}\frac{r^5}{a^6}-\frac{9}{32}\frac{r(r^2-a^2)^2}{a^6}\ln\left(\frac{r}{a}-1\right)\right\}\\
&+\epsilon^4X(1-X^2)\left\{\frac{1251}{768}\frac{r^2}{a^3}-\frac{2619}{2560}\frac{r^3}{a^4}-\frac{171}{256}\frac{r^4}{a^5}+\frac{2259}{15360}\frac{r^5}{a^6}+\frac{27}{512}\frac{r^7}{a^8}\right.\\
&\left.-\frac{171}{256}\frac{r^3(r^2-a^2)}{a^6}\ln\left(\frac{r}{a}-1\right)+\frac{63}{256}\frac{r(r^2-a^2)}{a^4}\ln\left(\frac{r}{a}-1\right)\right\}\\
&+\epsilon^4X^3(1-X^2)\left\{-\frac{261}{256}\frac{r^2}{a^3}+\frac{711}{2560}\frac{r^3}{a^4}+\frac{135}{256}\frac{r^4}{a^5}+\frac{1323}{5120}\frac{r^5}{a^6}-\frac{63}{512}\frac{r^7}{a^8}\right.\\
&\left.+\frac{135}{256}\frac{r^3(r^2-a^2)}{a^6}\ln\left(\frac{r}{a}-1\right)-\frac{27}{256}\frac{r(r^2-a^2)}{a^4}\ln\left(\frac{r}{a}-1\right)\right\}+O(\epsilon^6),
\end{aligned}
\tag{3.33}
$$

$$
X\equiv\frac{\sqrt{1-\epsilon^2}}{\epsilon}\sqrt{\frac{4a^2}{r^2}-1}. \tag{3.34}
$$

Although the functional form of $P(r;\epsilon)$ is different in the region $2b\leqslant r\leqslant 2a$ from what it is in the other regions, it can be shown that at the boundary of these two regions,

$$
\begin{aligned}
P_{\mathrm{I}}(2b;\epsilon)&=P_{\mathrm{II}}(2b;\epsilon)+O(\epsilon^6),\\
P'_{\mathrm{I}}(2b;\epsilon)&=P'_{\mathrm{II}}(2b;\epsilon)+O(\epsilon^4),
\end{aligned}
\tag{3.35}
$$

where the primes denote differentiation with respect to r. It is also straightforward to show that the expression for $P(r;\epsilon)$ given Eqs. (3.31)–(3.34) is appropriately normalized,

$$
\int_0^{2b}P_{\mathrm{I}}(r;\epsilon)\,dr+\int_{2b}^{2a}P_{\mathrm{II}}(r;\epsilon)\,dr=1+O(\epsilon^6). \tag{3.36}
$$

Figures 6 and 7 compare the analytic expressions found in Eqs. (3.31)–(3.34) to the results of

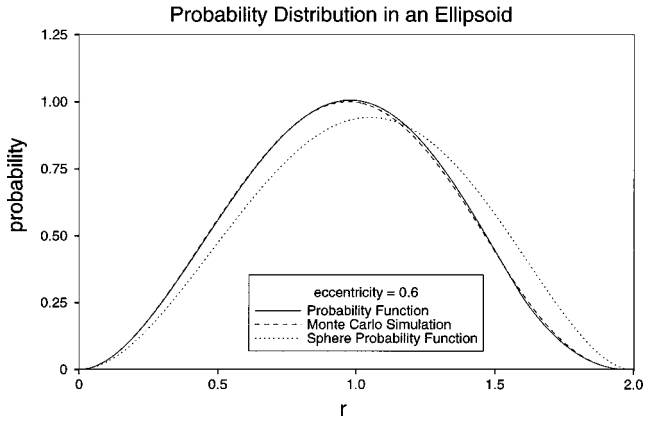

FIG. 7. A plot of the probability function $P_3(r;\epsilon)$ as a function of r for an ellipsoid with $a=1.0$ and $\epsilon=0.6$. Note that $P_3(r;\epsilon)$ in Eqs. (3.31)–(3.34) deviates slightly from the Monte Carlo simulation, shown by the dashed line, and that both of these curves differ from that for a sphere, shown by the dotted line.

a Monte Carlo simulation for different values of ϵ. For these simulations we have generated 10^9 random points in an oblate spheroid in which $a=1.0$ so that the largest possible distance between two points is 2.0. In addition the figures compare the results for $P_3(r;\epsilon)$ to those of a sphere with radius $a=1.0$. We see from these figures that the probability functions for an oblate spheroid are clearly different from those for a sphere. Moreover, the analytic results are seen to agree with those of the Monte Carlo simulation for $\epsilon \lesssim 0.6$. For larger values of ϵ higher powers of ϵ^2 would necessarily have to be included in our expansions.

IV. APPLICATIONS

We illustrate the application of our results in Eqs. (3.31)–(3.34), by using them to calculate the Coulomb energy of a charged ellipsoid. As noted in Sec. I, the significance of these results is that they allow $\langle V(r)\rangle \equiv U$ to be computed for an arbitrary two-body potential $V(r)$ in terms of a simple one-dimensional integral over the ellipsoidal matter or charge distribution. The Coulomb energy of an ellipsoidal nucleus has been found previously by Feenberg[18] using a different method, and we will show that our result agrees with that obtained in Ref. 18 to order ϵ^4. We find the Coulomb energy of a charged ellipsoid following the same procedure discussed in Sec. I. The potential energy of two charges, $e_1=e_2=e$, separated by a distance r is

$$V(r)=\frac{e^2}{|\mathbf{r}_1-\mathbf{r}_2|}=\frac{e^2}{r}, \tag{4.1}$$

and the probabilities of finding these charges at $\mathbf{r}_1$ and $\mathbf{r}_2$ are $\rho_1 d^3r_1$ and $\rho_2 d^3r_2$, respectively, where

$$\rho_1=\rho_2=\rho_0=\frac{1}{\frac{4}{3}\pi a^3\sqrt{1-\epsilon^2}}. \tag{4.2}$$

It follows that the potential energy between two such charges in an ellipsoid of uniform charge density is

$$dU=(\rho_0 d^3r_1)(\rho_0 d^3r_2)V(|\mathbf{r}_1-\mathbf{r}_2|). \tag{4.3}$$

As in the case of a spherical matter or charge distribution, the average potential energy is found by integrating over all possible $\mathbf{r}_1$ and $\mathbf{r}_2$ in the ellipsoid, which necessitates the evaluation of a

nontrivial six-dimensional integral. By contrast, the present formalism allows the same calculation to be carried out as a one-dimensional integral using the ellipsoid probability function. Since U is the average electrostatic energy, it may be written as

$$U=\langle V(r)\rangle_{\text{ellipsoid}}=\int_0^{2a}P(r)V(r)\,dr=\int_0^{2b}P_{\text{I}}(r)V(r)\,dr+\int_{2b}^{2a}P_{\text{II}}(r)V(r)\,dr, \tag{4.4}$$

where $P_{\text{I}}(r)$ and $P_{\text{II}}(r)$ are the probability functions for each region of r and are given by Eqs. (3.32) and (3.33), respectively. The integrals in Eq. (4.4) can be evaluated in a straightforward manner and, after expanding the results in powers of ϵ, we find to order ϵ^4

$$U=\frac{6}{5}\frac{e^2}{a}\left\{1+\frac{1}{6}\epsilon^2+\frac{3}{40}\epsilon^4+O(\epsilon^6)\right\}. \tag{4.5}$$

Equation (4.5) gives the energy U for a single pair of charges. Since a nucleus which contains Z charges can form $Z(Z-1)/2$ pairs, it follows that the Coulomb energy W_C of a charged ellipsoid to order ϵ^4 is

$$W_C=\frac{3}{5}\frac{Z^2e^2}{a}\left\{1+\frac{1}{6}\epsilon^2+\frac{3}{40}\epsilon^4+O(\epsilon^6)\right\}, \tag{4.6}$$

where $Z(Z-1)$ has been approximated by Z^2. The result of Eq. (4.6) can be compared to Feenberg's calculation[18] of the Coulomb energy of a perturbed nucleus. Feenberg assumes that the nucleus is perturbed from its original spherical shape to an ellipsoid defined by

$$x^2+y^2+\left(\frac{z}{\bar{a}}\right)^2=\frac{R^2}{\bar{a}^{2/3}}, \tag{4.7}$$

where R is the radius of the unperturbed nucleus. Note that in the above parametrization of an ellipsoid the volume of the nucleus is always $4\pi R^3/3$ independent of $\bar{a}$. When the nucleus is perturbed, Feenberg finds for the Coulomb energy

$$W_C=\frac{3}{5}\frac{Z^2e^2}{R}\left\{1-\frac{4}{45}(\bar{a}-1)^2+\cdots\right\}. \tag{4.8}$$

To compare Eqs. (4.6) and (4.8) we note that the equation for the ellipsoid in Eq. (3.1),

$$\frac{x^2}{a^2}+\frac{y^2}{a^2}+\frac{z^2}{b^2}=1, \tag{4.9}$$

can be written as

$$x^2+y^2+\left(\frac{z}{\sqrt{1-\epsilon^2}}\right)^2=a^2, \tag{4.10}$$

where we have replaced b with $a\sqrt{1-\epsilon^2}$. Comparing Eqs. (4.10) and (4.7), we see that

$$\bar{a}=\sqrt{1-\epsilon^2}, \tag{4.11}$$

$$R=a(1-\epsilon^2)^{1/6}. \tag{4.12}$$

Combining Eqs. (4.8), (4.11), and (4.12), we find

$$W_C=\frac{3}{5}\frac{Z^2e^2}{a(1-\epsilon^2)^{1/6}}\left\{1-\frac{4}{45}(\sqrt{1-\epsilon^2}-1)^2+\cdots\right\}. \tag{4.13}$$

Expanding Eq. (4.13) in a Taylor series about $\epsilon=0$, we find

$$W_C=\frac{3}{5}\frac{Z^2e^2}{a}\left\{1+\frac{1}{6}\epsilon^2+\frac{3}{40}\epsilon^4+O(\epsilon^6)\right\}. \tag{4.14}$$

This is exactly the same result that was found in Eq. (4.6) by using the ellipsoid probability function.

We note in passing that although it may appear from Eq. (4.14) that the Coulomb energy of the ellipsoid is larger than that of the original sphere, this is not the case. Recall that the unperturbed nucleus has a Coulomb energy given by

$$W_C^{\text{sphere}}=\frac{3}{5}\frac{Z^2e^2}{R}. \tag{4.15}$$

When this is compared to the leading term in Eq. (4.14), we observe that

$$\frac{3}{5}\frac{Z^2e^2}{R}>\frac{3}{5}\frac{Z^2e^2}{a} \tag{4.16}$$

since $R<a$. Even though it seems as though more terms are being added to the original energy, this is not the case since the leading term in Eq. (4.14) is not the original energy. In fact, if we replace a with $R(1-\epsilon^2)^{-1/6}$ in Eq. (4.14), and then expand the result in a Taylor series, we find that the Coulomb energy *decreases* as a result of perturbing the nucleus from its original spherical shape.

ACKNOWLEDGMENTS

We are deeply indebted to Professor A. W. Overhauser for making his unpublished results available to us, and for numerous discussions. We also wish to thank David Schleef, Shu-Ju Tu, Brian Woodahl, and Michael Yurko for helpful conversations. This work was supported in part by the U.S. Department of Energy under Contract No. DE-AC-02-76 ERO 1428.

APPENDIX: DISTRIBUTION OF DISTANCE IN A ELLIPSE

We present in this Appendix the probability distribution of distance in an ellipse. The previous formalism can be taken over immediately to obtain $P_2(r;\epsilon)$ for an ellipse, as discussed in Ref. 15, and hence only the final results are presented here. We find

$$P_2(r;\epsilon)=\begin{cases}P_{2\mathrm{I}}(r;\epsilon), & 0\leqslant r\leqslant 2b,\\ P_{2\mathrm{II}}(r;\epsilon), & 2b\leqslant r\leqslant 2a,\end{cases} \tag{A1}$$

$$\begin{aligned}P_{2\mathrm{I}}(r;\epsilon)=\frac{1}{\pi a}\Bigg\{&8\left[\left(\frac{r}{2a}\right)\cos^{-1}\left(\frac{r}{2a}\right)-\left(\frac{r}{2a}\right)^2\sqrt{1-\left(\frac{r}{2a}\right)^2}\right]+4\epsilon^2\Bigg[\left(\frac{r}{2a}\right)\cos^{-1}\left(\frac{r}{2a}\right)\\&-2\left(\frac{r}{2a}\right)^2\sqrt{1-\left(\frac{r}{2a}\right)^2}\Bigg]+3\epsilon^4\Bigg[\left(\frac{r}{2a}\right)\cos^{-1}\left(\frac{r}{2a}\right)-3\left(\frac{r}{2a}\right)^2\sqrt{1-\left(\frac{r}{2a}\right)^2}\\&+\frac{1}{4}\left(\frac{r}{2a}\right)^2\left(1-\left(\frac{r}{2a}\right)^2\right)^{-1/2}\Bigg]\Bigg\},\end{aligned} \tag{A2}$$

$$
\begin{aligned}
P_{2\mathrm{II}}(r;\epsilon)=\frac{4}{\pi^2 a}\left(\frac{r}{2a}\right)\Bigg\{&\left[\cos^{-1}\left(\frac{r}{2a}\right)-\left(\frac{r}{2a}\right)\sqrt{1-\left(\frac{r}{2a}\right)^2}\right]4\cos^{-1}(X)\\
&+\epsilon^2\Bigg[2\cos^{-1}\left(\frac{r}{2a}\right)\{\cos^{-1}(X)+X\sqrt{1-X^2}\}-2\left(\frac{r}{2a}\right)\sqrt{1-\left(\frac{r}{2a}\right)^2}\\
&\otimes\{2\cos^{-1}(X)+X\sqrt{1-X^2}\}-2\left(\frac{r}{2a}\right)^2\left[\cos^{-1}\left(\frac{r}{2a}\right)-\cos^{-1}\left(\frac{r^4-3r^2a^2}{2ra^3}\right)\right]\\
&\otimes\{X\sqrt{1-X^2}\}-\frac{1}{2}\left[\cos^{-1}\left(\frac{r}{2a}\right)+\cos^{-1}\left(\frac{r^4-3r^2a^2}{2ra^3}\right)\right]\{X\sqrt{1-X^2}\}\Bigg]\\
&+\epsilon^4\Bigg[\cos^{-1}\left(\frac{r}{2a}\right)\left\{\frac{3}{2}\cos^{-1}(X)+\frac{3}{2}X\sqrt{1-X^2}+X^3\sqrt{1-X^2}\right\}\\
&-\frac{r}{2a}\sqrt{1-\left(\frac{r}{2a}\right)^2}\left\{\frac{9}{2}\cos^{-1}(X)+2X\sqrt{1-X^2}\right\}+\left(\frac{r}{2a}\right)^3\sqrt{1-\left(\frac{r}{2a}\right)^2}\{3X\sqrt{1-X^2}\\
&-6X^3\sqrt{1-X^2}\}+\left(\frac{r}{2a}\right)\frac{1}{\sqrt{1-(r/2a)^2}}\left\{\frac{3}{8}\cos^{-1}(X)-\frac{5}{8}X\sqrt{1-X^2}+\frac{1}{4}X^3\sqrt{1-X^2}\right\}\\
&-2\left(\frac{r}{2a}\right)^2\left[\cos^{-1}\left(\frac{r}{2a}\right)-\cos^{-1}\left(\frac{r^4-3r^2a^2}{2ra^3}\right)\right]\otimes\{X\sqrt{1-X^2}+X^3\sqrt{1-X^2}\}\\
&-\frac{1}{2}\left[\cos^{-1}\left(\frac{r}{2a}\right)+\cos^{-1}\left(\frac{r^4-3r^2a^2}{2ra^3}\right)\right]\left\{\frac{3}{4}X\sqrt{1-X^2}+\frac{1}{2}X^3\sqrt{1-X^2}\right\}\Bigg]\Bigg\},
\end{aligned}
\tag{A3}
$$

where

$$
X=\frac{1}{\epsilon}\sqrt{1-\frac{4a^2}{r^2}(1-\epsilon^2)}. \tag{A4}
$$

[1] A. Bohr and B. R. Mottelson, *Nuclear Structure* (Benjamin, New York, 1969), Vol. 1.
[2] F. Ferrer and J. A. Grifols, Phys. Rev. D **58**, 096006 (1998).
[3] V. M. Mostepanenko and I. Yu. Sokolov, Sov. J. Nucl. Phys. **46**, 685 (1987).
[4] S. D. Drell and K. Huang, Phys. Rev. **91**, 1527 (1953).
[5] E. Fischbach and D. Krause, Phys. Rev. Lett. **82**, 4753 (1999); **83**, 3593 (1999).
[6] D. Sudarsky, C. Talmadge, and E. Fischbach (unpublished).
[7] G. Feinberg and J. Sucher, Phys. Rev. **166**, 1638 (1968); G. Feinberg, J. Sucher, and C.-K. Au, Phys. Rep. **180**, 83 (1989).
[8] J. B. Hartle, Phys. Rev. D **1**, 394 (1970).
[9] S. D. H. Hsu and P. Sikivie, Phys. Rev. D **49**, 495 (1994).
[10] E. Fischbach, Ann. Phys. (N.Y.) **247**, 213 (1996); E. Fischbach and C. Talmadge, *The Search for Non-Newtonian Gravity* (AIP/Springer, New York, 1999).
[11] R. Deltheil, Ann. Fac. Sci. Univ. Toulouse **11** (3), 1 (1919).
[12] J. M. Hammersley, Ann. Math. Stat. **21**, 447 (1950).
[13] A. Overhauser (1950), unpublished.
[14] R. D. Lord, Ann. Math. Stat. **25**, 794 (1954).
[15] M. Parry, ''Application of Geometric Probability Techniques to Elementary Particle and Nuclear Physics,'' Ph.D. thesis, Purdue University, 1998 (unpublished).
[16] M. G. Kendall and P. A. P. Moran, *Geometric Probability* (Hafner, New York, 1963).
[17] L. A. Santaló, *Integral Geometry and Geometric Probability* (Addison-Wesley, Reading, MA, 1976).
[18] E. Feenberg, Phys. Rev. **55**, 504 (1939).